Biocybernetics and Biomedical Engineering 45 (2025) 278–286

Contents lists available at ScienceDirect

Biocybernetics and Biomedical Engineering

journal homepage: www.elsevier.com/locate/bbe

Research Paper

Validation of a markerless motion capture system for centre of mass kinematic analysis

Ruben Valenzuela [a,*], Javier Corral [a], Mikel Diez [a], Thomas Provot [b,c], Francisco J. Campa [a], Saioa Herrero [a], Erik Macho [a], Charles Pinto [a]

[a] Bilbao School of Engineering, Plaza Ingeniero Torres Quevedo 1, Bilbao, 48013, Biscay, Spain
[b] EPF–Engineering School, 55 Avenue du Président Wilson, Cachan, 94230, Paris, France
[c] Arts et Métiers Institute of Technology, Institut de Biomécanique Humaine Georges Charpak, IBHGC, UR 4494, 75013 Paris, France, Université Sorbonne Paris Nord, 3000 Bobigny, France

ARTICLE INFO

Keywords:
Centre of mass
Markerless vs Marker-based
Pose estimation
Bland–Altman plot

ABSTRACT

In recent years, markerless optical systems for biomechanical movement analysis in sports, gait and balance assessments are being used as an alternative to conventional marker based measuring systems. This study compares the performance of the Zed 2i stereoscopic camera against a VICON system in a standing position under three conditions: quiet standing and two movements simulating disturbances in two directions, anteroposterior and mediolateral. This study originates from a collaborative project with a medical team that aims to objectively evaluate balance function in patients recovering from stroke. The displacement and velocities of the centre of mass were calculated and compared in two directions, x and y. A Bland–Altman analysis for non-parametric data, along with the coefficient of determination and mean square error, were used for statistical evaluation. The results demonstrate that the limits of agreement in both sway tasks were greater than those observed in static conditions. However, the coefficient of determination of the sway tasks indicates a significant degree of agreement between the two systems. In contrast, in the static condition, it appears that noise may have a greater influence on the signal than the centre of mass estimate, due to the limitation of the depth algorithm used to estimate the joint positions.

1. Introduction

Balance is a fundamental function of daily activities that involves synergy of the vestibular, visual, and somatosensory systems [1]. These sensory inputs are processed by the central nervous system, which generates the required strategies to maintain the centre of mass (COM) within the limits of the base of support (BOS) [2]. Balance is clinically assessed through different standardised tests such as the Timed Up & Go [3] or the Berg Balance Scale, among others [4]. A more quantitative measurement of balance is static or dynamic posturography, or stabilometry, which focuses on measuring the centre of pressure (COP) with a dynamometric platform or force plate. The COP is defined as the location, within the BOS, where the total reaction force on the ground acting on a person's foot or feet is concentrated [5]. The study and analysis of the relationship between these parameters have been conducted to characterise the behaviour of balance and to quantitatively identify the variations that can occur under various conditions [6–9]. Some of these studies include: diagnosis and prevention of falls in older people [10], Parkinson's disease [11], and people with chronic obstructive pulmonary disease [12]. Furthermore, COM behaviour and its relationship with COP have also been used to study the effects of ageing and hemiplegia [13], and to discriminate between elderly fallers and non-fallers [14], proving to be a valuable asset in the study of the intricacies of balance and postural control. Other research studies have also identified that the velocity of the COM can be used in balance assessment to identify potential fall risks in elder people [15] and the relationship between movement of different body segments and the COM velocity with posture instability [16].

However, estimating the COM position presents a great challenge, since it cannot be directly measured. A first approach is to measure the masses and lengths of each subject segments to calculate their total COM [17]. This is not only impractical, but also time consuming, therefore other methods for its estimation were developed, such as double integration of the COP [18], low-pass filter of the COP [19], Inertial Measurement Unit (IMU) based estimations [20,21], and videogrammetry, the last acknowledged as the gold standard [22].

Measurement by videogrammetry, commonly known as motion capture (Mocap), is mostly performed with specialised equipment, such as

* Correspondence to: Plaza Ingeniero Torres Quevedo 1, Bilbao, 48013, Biscay, Spain.
E-mail address: ruben.valenzuela@ehu.eus (R. Valenzuela).

https://doi.org/10.1016/j.bbe.2025.03.004
Received 18 October 2024; Received in revised form 26 March 2025; Accepted 28 March 2025
Available online 21 April 2025

optoelectronic systems based on reflective markers. These markers are placed on key anatomical landmarks of a patient and infrared cameras are used to track the movement along a recording space [23]. This system has been used to measure gait patterns and speeds [24,25], as well as gait disturbances due to different diseases such as rheumatoid arthritis [26]. Another study tracked the behaviour of individuals with hip osteoarthritis [27] where fourteen markers were placed on the sacrum and on both iliac crests, and other key bony landmarks to measure hip flexion–extension. Other uses are related to the study of sports biomechanics, such as football [28] or handball [29] motions. While precise, this method is not without flaws as it requires strict experimental conditions such as a suitable conditioned space, multiple cameras for proper tracking which in turn increases the price restricting its accessibility, and specialised training for proper marker placement to accurately compute the COM. Additionally, even under optimal conditions, marker placement can generate errors due to soft tissue artefacts [30]. Marker placement is also time consuming, making it difficult to handle long measurement sessions for healthcare applications.

Recently, there has been an increase in the use of markerless systems for human pose estimation. These systems employ images or videos acquired by single or multi-camera setups to estimate the position of joint coordinates through convolutional neural networks, removing the need to attach reflective markers [31]. Research on single camera systems such as the Microsoft Kinect v2 has been explored in telemedicine for remote health monitoring [32]) and compared COM estimates with double integration of the COP method [33]. Although these works highlight the potential of markerless systems, the validation methods of Root Mean Square Error (RMSE) values and/or Pearson's coefficient of correlation have limitations. RMSE provides a summary of the overall error, but does not identify when it occurs during motion, it neither identifies whether it is systematic or random. Similarly, the Pearson correlation coefficient often yields high values when the compared systems measure the same parameter, regardless of whether their outputs differ systematically [34]. To address these issues, a Bland–Altman analysis is recommended to better assess the agreement and performance of these systems, as well as the type of error present between both measurement systems [35].

Other studies have compared the performance of multi-camera markerless and marker-based technologies through different static and dynamic motions. Some researchers focus on kinematic variables such as pelvic tilt, hip flexion, and ankle eversion. In these studies, markerless systems, despite certain limitations such as lower accuracy or difficulties to correctly measure patients with certain deformities, show promise in clinical and rehabilitation environments due to their ease of use [36,37]. A different study measured the agreement in COM estimation applying a Bland–Altman analysis to several parameters derived from the COM through dynamic motions [38]. While these multi-camera systems are cheaper than their marker-based counterparts, their high cost still limits their accessibility. Additionally, multi-camera setups require technical expertise for calibration and installation.

A different approach to 2D image estimation is the use of stereoscopic cameras, such as the Zed 2i. Unlike monocular cameras, which are limited to 2D estimation, stereoscopic cameras provide 3D depth, enabling new possibilities for pose estimation research [39]. This technology employs two optical sensors to estimate object depth. With this feature and the use of neural networks, the positions of several keypoints related to anatomic joints can be identified. The use of a single camera enhances adaptability, as it can be used in different space conditions. This flexibility allows it to be used with mobile dynamometric platforms [40], which facilitates a detailed analysis of the relationship between COP and COM. However, despite its advantages, markerless systems have drawbacks, including lower accuracy and robustness compared to marker-based systems [41]. After an in-depth state of the art research we consider that there has been limited research on stereoscopic cameras for COM estimation in balance studies.

Table 1
Participant characteristics.

Parameter	Value
Number of participants (n)	8
Age (years)	35.6 ± 4.87
Mass (kg)	77.0 ± 12.05
Height (cm)	180.7 ± 8.96

The aim of this study is to validate the COM estimation of the Zed 2i markerless model by comparing it to a marker-based optoelectronic system, considered the gold standard, using anthropometric tables. Specifically, we evaluate two distinct models: the marker-based model, which employs Dumas anthropometric tables [42], and a simplified nine-segment model derived from the Zed 2i pose estimation algorithm, which utilises Winter anthropometric tables [43]. The assessment is conducted using simple movements such as quiet standing, and anteroposterior and mediolateral oscillations, which simulate maintaining balance, without altering the BOS, after suffering a disturbance. These movements emulate the behaviour of a mobile dynamometric platform, which are designed to assess balance of elderly adults, stroke patients, Parkinson's disease, or multiple sclerosis patients. [44–46]. Finally, this study evaluates the feasibility of the Zed 2i as a low-cost auxiliary tool in biomedical and clinical applications where balance assessment through posturography is evaluated.

2. Materials and methods

2.1. Experimental protocol

Eight healthy male participants were selected for this study (Table 1), all of whom gave their informed consent in accordance with the Declaration of Helsinki [47]. Approval of all ethical and experimental procedures and protocols was granted by the CPP Sud-Ouest et Outre-Mer I et II under Application No. 2020-A01357-32. Participants wore minimal clothing to facilitate proper marker placement and a full-body marker set, consisting of 52 markers, was placed according to Dumas anthropometric tables to estimate the COM [42].

Movements were measured using a VICON system (Vicon, Oxford, UK) composed of fourteen VERO 2.2 cameras (250 Hz @ 2.2 MP Sensors) and simultaneously captured by a Zed 2i camera (Stereolabs, San Francisco, CA, US) (30 Hz @ 2 x 4 MP Sensors, SDK ver. 4.0.6). The VICON system was calibrated according to the specifications provided in the user manual to provide a global reference frame (O-XYZ). The Zed 2i camera was placed on a tripod 2 metres from the participant, at a height of 90 cm, and orientated at an oblique angle of −10 degrees with respect to the sagittal plane. This setup was defined to measure the overall performance of the pose estimation algorithm. Additionally, a custom-made hat with three markers was placed on the Zed 2i camera to determine its position within the VICON recording space for post-process spatial alignment of the marker-based and markerless models. This hat was specifically designed to have the centre of the generated reference frame located 6 cm to the right and 2.5 cm above the internal reference frame of the camera (Zed-XYZ), the centre of which is located at the left optical sensor.

The equipment used to acquire the measurements of the Zed 2i camera was a ROG Zephyrus G14 (ASUS, Taipei, Taiwan) with an AMD Ryzen 5900HS CPU (AMD, CA, US) and a GeForce RTX 3050 Ti GPU (Nvidia, CA, US). The mass of each subject was calculated using the reaction force in z with the triaxial AMTI dynamometric platforms (Advanced Mechanical Technology Inc, MA, USA).

The experimental protocol consisted of an initial static measurement to reconstruct the VICON model for post processing, and three sets of tasks, each performed with feet placed at shoulder width and arms in anatomical position. The tasks included ten static repetitions of five seconds duration, ten repetitions of an anteroposterior sway movement

starting in the anterior direction, and ten repetitions of a mediolateral sway movement starting in the right mediolateral direction. To ensure repeatability between tests, participants were instructed to avoid raising the toes or heel from the ground during the sway movements, additionally, the trunk was to remain aligned with the pelvis without flexion. This resulted in a variable test duration ranging from thirty to forty seconds. Finally, since both measurements were acquired independently, an elbow flexion was performed at the end of each trial to synchronise both models during post-processing.

3. Data processing

3.1. Marker-based system

Marker-based data were acquired, reconstructed, labelled, and processed using Nexus software version 2.14 (Vicon, Oxford, UK). The obtained marker positions were imported into MATLAB (Mathworks, Natick, MA, US) to estimate the position of the COM. Based on Dumas et al. anthropometric table, the body was modelled as a 16-segment model (head, thorax, abdomen, pelvis, upper arms, forearms, hands, thighs, shanks, and feet), estimating the position of the COM and mass of each segment (Fig. 1(a)) from the 52 markers mentioned in Section 2.1. First, the following joint centres were computed:

- Bilateral Joint Centres
  - Ankles
  - Knees
  - Hips
  - Shoulders
  - Elbows
  - Wrists
- Vertebral Column Joints Centres
  - Lumbar
  - Thoracic
  - Cervical

$$\overrightarrow{COM}_T = \frac{\sum_{i=1}^{n}(\overrightarrow{COM}_i \cdot m_i)}{M}. \quad (1)$$

Afterwards, the local coordinate systems for each segment were calculated using the markers placed around the joints, and finally, the COM position for each segment was obtained (shown as black dots in Fig. 1). To compute the total COM ($\overrightarrow{COM}_T$) (Shown as a green dot in Fig. 1), Eq. (1) was used:

Where $\overrightarrow{COM}_i, i = 1...16$ the position of the segment i COM with respect to O-XYZ, m_i the mass of the segment i, and M is the total mass of the body. In these equations, the mass of each segment is estimated using Dumas et al. anthropometric tables, which define each segment as a percentage of the total body mass.

3.2. Markerless system

The Zed 2i camera detects depth using stereoscopic technology by computing the displacement between pixels acquired by the left and right cameras [48]. The depth range extends from 0.2 to 20 metres, and the camera has a field of view of 110 degrees. The pose estimation algorithm uses a convolutional neural network for keypoint detection and, in conjunction with the depth estimation, provides the 3D position of each keypoint. Each keypoint corresponds to an anatomical joint. The Zed 2i pose estimation algorithm provides three different models, each with a number of keypoints. For this study, a thirty-eight keypoint body format was used as this model provides the joint centre positions for bilateral wrists, elbows, shoulders, ankles, knees, hips, pelvis, and three keypoints corresponding to the thorax, resulting in a

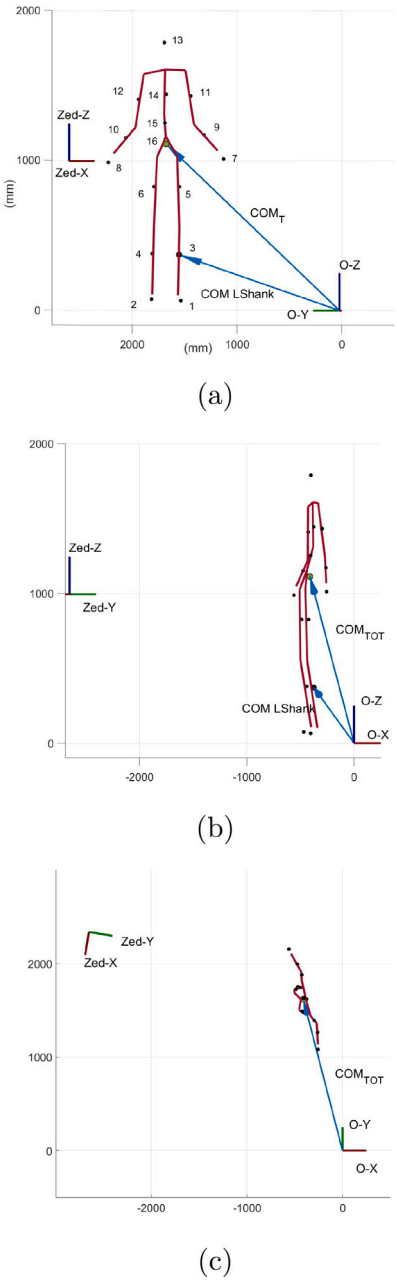

Fig. 1. VICON model (a) Front view (b) Side view (c) Top view.

nine-segment model (Fig. 2(a)). Data acquisition was performed using a custom Python script in which a Z-Up right-handed coordinate system was defined, where the y-axis points towards the camera lens, the x-axis points to the right, and the z-axis points upwards.

Since the provided keypoints were insufficient to accurately determine the local coordinate systems for each segment and compute its COM position, the Dumas methodology cannot be applied. Due to this limitation, Winter anthropometric tables [43] were used, as this method estimates the COM position of the segment along the vector that connects two joint centres. The model used includes nine segments: bilateral shank and foot, thigh, forearm and hand, upper arm, trunk, and neck-head, leading to the corresponding nine COM in Fig. 2(a). For the total COM, Eq. (1) was used, adjusted for the number of segments in the markerless model ($i = 1...9$).

To compare both models, a transformation matrix was applied to the Zed 2i model so that the data were expressed in terms of the global

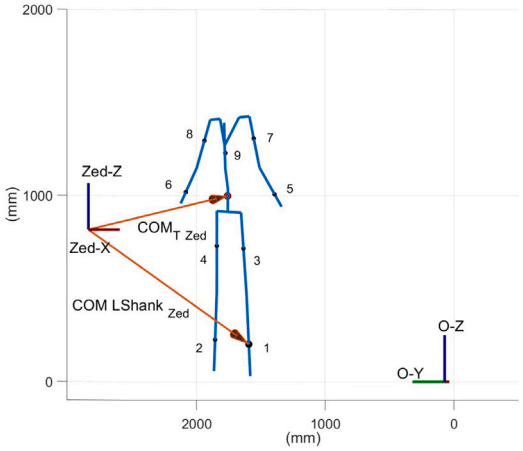

Fig. 2. Zed 2i model (a) Front view (b) Side view.

reference system Eq. (2):

$$P^{O}_{Zed} = \boldsymbol{T}^{O}_{Zed} \cdot P_i. \tag{2}$$

$$\boldsymbol{T}^{O}_{Zed} = \begin{bmatrix} \boldsymbol{R}_{Zed} & d_{Zed} \\ 0 & 1 \end{bmatrix}. \tag{3}$$

Where $\boldsymbol{R}_{Zed}$ is the rotation matrix of the Zed 2i coordinate reference system Zed-XYZ in the global reference frame, d_{Zed} is the position vector of the internal Zed 2i camera reference system, after adjusting the offset of the marker hat, relative to the reference global frame, and $P_i, i = 1...38$ the position of each keypoint in space with respect to Zed-XYZ, and P^{V}_{Zed} is the position of the keypoints in space with respect to O-XYZ.

In Fig. 3 the initial position of a participant is shown after applying the transformation matrix, where O-XYZ is the global reference frame and Zed-XYZ is the Zed 2i internal camera reference frame.

3.3. Signal processing

Data acquired by the Zed 2i camera experienced a variable sampling frequency drop from 25 Hz to 5 Hz towards the end of the trials, we identified that this was caused by the used hardware, more specifically, the graphics card. To achieve a constant sample rate of

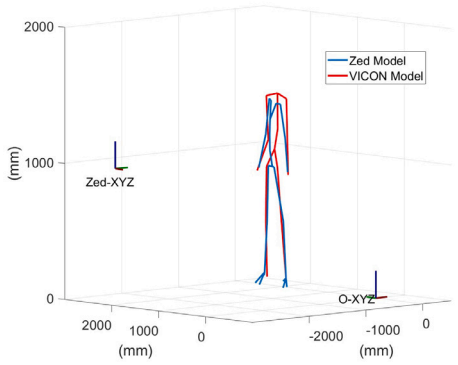

Fig. 3. Spatial alignment of both models, isometric view.

50 Hz for analysis, a cubic spline interpolation during post-process was applied. To compare both signals, data acquired by the VICON system were downsampled to 50 Hz. The elbow flexion angle was computed with the marker-based and markerless kinematic models, and filtered using a zero-phase low-pass fourth-order Butterworth filter with a cutoff frequency of 5 Hz. After filtering, the maximum value of the elbow flexion, computed with both the marker-based system and the markerless system, was synchronised.

The positions of both estimated total COM were filtered through a zero-phase low-pass fourth-order Butterworth filter with a variable cut-off frequency determined through the residual analysis method [43], where the second derivative of the residual curve was calculated. A threshold, consisting of the mean value of the second derivative curve, was used to identify the frequency at which the most abrupt increase occurred. This frequency was used as the optimal cut-off frequency [49]. To compute the velocity, a Matlab derivative algorithm was applied to the COM position in the x and y directions.

3.4. Statistical analysis

To maintain the consistency of the comparisons, the elbow flexion event was removed from the signal analysis. For the static task we used the first four seconds. In terms of sway exercises, the time interval between the first and last maxima of the predominant movement was used to ensure this consistency.

The comparison between both systems was based on the displacement and velocity of the COM in the x and y directions of the global reference frame.

To assess the level of agreement between the two measurement systems, a Bland–Altman analysis between measurement methods with multiple observations per repetition was applied (observations varying from 200 for static tasks to [1000 - 1300] for sway tasks) [50]. Bland–Altman analysis assumes that the distribution of differences is normally distributed. However, upon applying the Kolmogorov–Smirnov test to the data, it was found that this assumption was not met, and thus the data can be classified as non-parametric. Therefore, to calculate the limits of agreement (LOA), the quantile method [51] was used, ensuring that 95% of the total dataset fell within these LOA. The root mean square error (RMSE) and the coefficient of determination R^2 were also calculated. R^2 indicates the strength of the linear relationship between the two measures. The classification used for R^2 was: weak ($R^2 < 0.4$), moderate ($0.4 < R^2 < 0.7$), significant ($0.7 < R^2 < 0.9$) and substantial ($R^2 > 0.9$).

The values presented for the displacement analysis are calculated after a mean de-trend and with respect to the origin of the coordinate system, since the indicators used in posturography are often calculated relative to the mean value of the COP/COM [7].

Table 2
Bland–Altman analysis for each task and across all tasks, for all participants.

Indicator	Parameter	Static		AP Sway		ML Sway	
		x	y	x	y	x	y
Displacement (mm)	LOA (lower)	−4.54	−2.01	−17.93	−9.84	−11.49	−14.34
	LOA (upper)	3.88	2.06	17.56	9.46	11.45	14.96
	RMSE	2.13	1.06	9.41	5.10	5.99	7.70
	R^2	0.46	0.26	0.94	0.85	0.92	0.98
Velocity (mm/s)	LOA (lower)	−8.33	−5.00	−42.71	−22.76	−30.34	−39.88
	LOA (upper)	10.65	4.66	44.65	23.36	29.57	41.64
	RMSE	4.78	2.63	23.49	12.53	15.54	20.17
	R^2	0.13	0.08	0.92	0.83	0.91	0.98

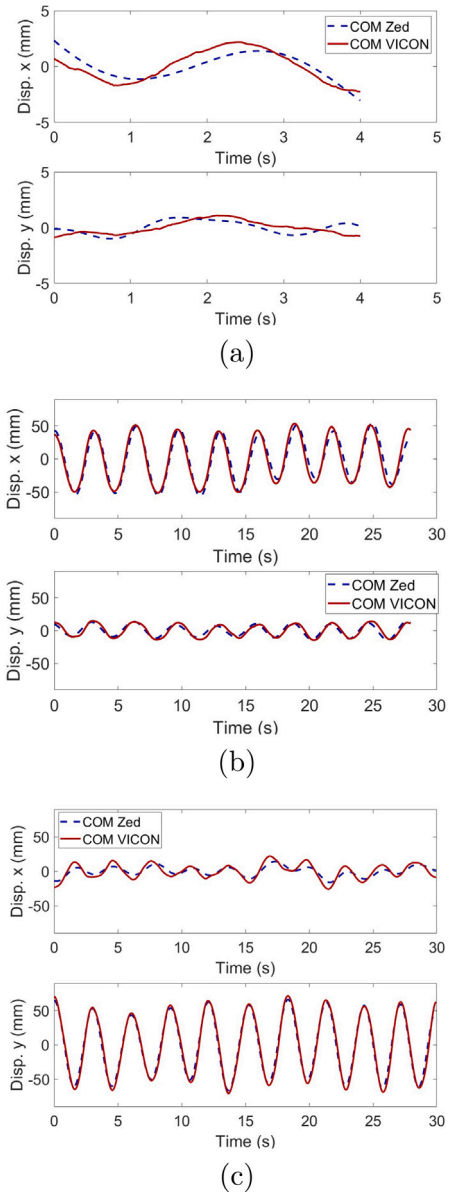

Fig. 4. Signal behaviour in x and y directions for: (a) Static task, (b) AP sway task, (c) ML sway task.

4. Results

A number of measurements were lost due to inadequate recording of the synchronisation event or unexpected behaviours in the measurements. These incomplete datasets were excluded from the error index calculations, three of which were of the static test, two of the AP sway tests, and one of the ML sway tests. As a result, 77 static tests, 78 AP sway tests, and 79 ML sway tests were analysed.

In Fig. 4 the comparison of both COM displacement estimation in both directions for each exercise and a different participant is shown. It can be seen that the COM behaviour of both models in sway exercises is more similar than the static exercises, particularly in the predominant movement direction.

4.1. COM displacement

Various patterns of differences between conditions can be identified by the Bland–Altman analysis (Fig. 5). In static condition, a greater error was observed in the x direction compared to the y direction, as evidenced by the broader LOA and higher RMSE shown in Table 2. For sway tasks, the difference was higher in the predominant movement direction, that is, the x direction for the AP sway and the y direction for the ML sway. R^2 indicates moderate agreement in static tests for the x direction (0.49) and weak for the y direction (0.29). While, for the sway tasks R^2 were substantial and strong for AP sway in x and y directions respectively (0.94, 0.85) and substantial for both directions in ML direction. These values indicate a strong agreement with the gold standard behaviour, supporting the Zed 2i camera's model effectiveness for dynamic posturography assessments. It is important to note that the LOA and RMSE obtained fall within the depth error range reported by Ortiz et al. [48], which found a mean error of 0.2 m and a variance of 0.12 m.

4.2. COM velocity

Bland–Altman velocity analysis revealed similar trends (Fig. 6). For static trials, the difference was greater in the x direction, as indicated by the broader LOA and larger RMSE for the x direction (4.78 mm/s) compared to the y direction (2.63 mm/s). In sway conditions, the LOA were broader and the RMSE was higher in the predominant direction, which is the x direction for the AP sway and the y direction for the ML sway. Regarding the R^2 coefficient, the x and y directions have a weak correlation, both significantly lower than the displacement. However, R^2 coefficients of sway movements remain consistent with the displacement coefficients, further indicating that the Zed 2i camera performs better in dynamic conditions.

5. Discussion

The aim of this study is to measure the accuracy of the Zed 2i markerless system against a gold standard reference system (VICON) while performing balance related tasks without altering the BOS. Measuring and estimating the COM is fundamental for understanding the relationship between COM and the COP, as well as the intrinsic mechanisms underlying postural control [52,53]. In dynamic posturography, mobile dynamometric platforms are often used to apply external perturbations. However, these perturbations complicate COM estimation by affecting analytic methods such as low-pass filtering [54]. As a result, vision-based systems are preferred as an alternative to accurately capture COM

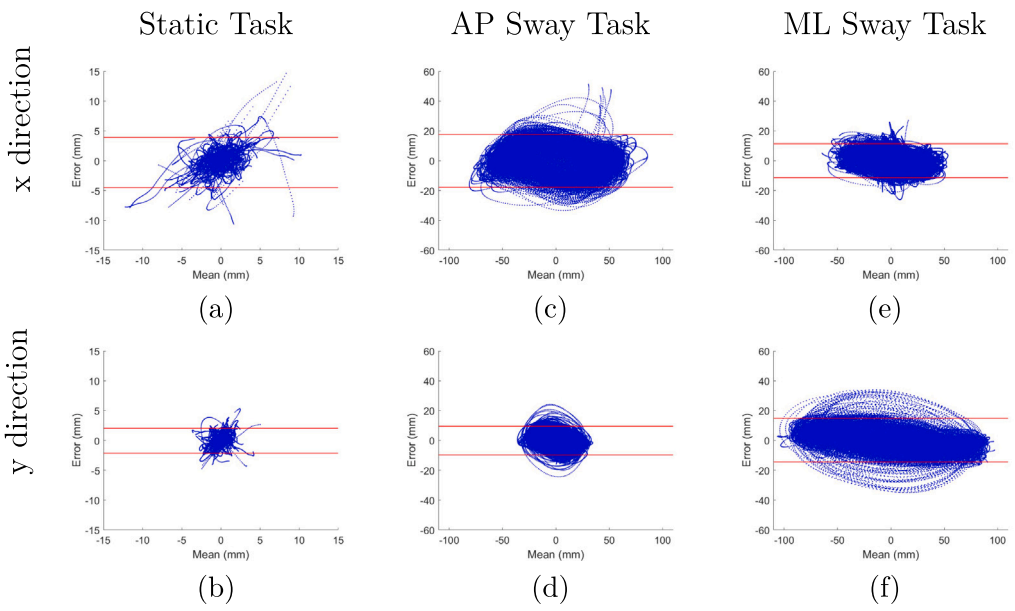

Fig. 5. Bland–Altman plots for displacement.

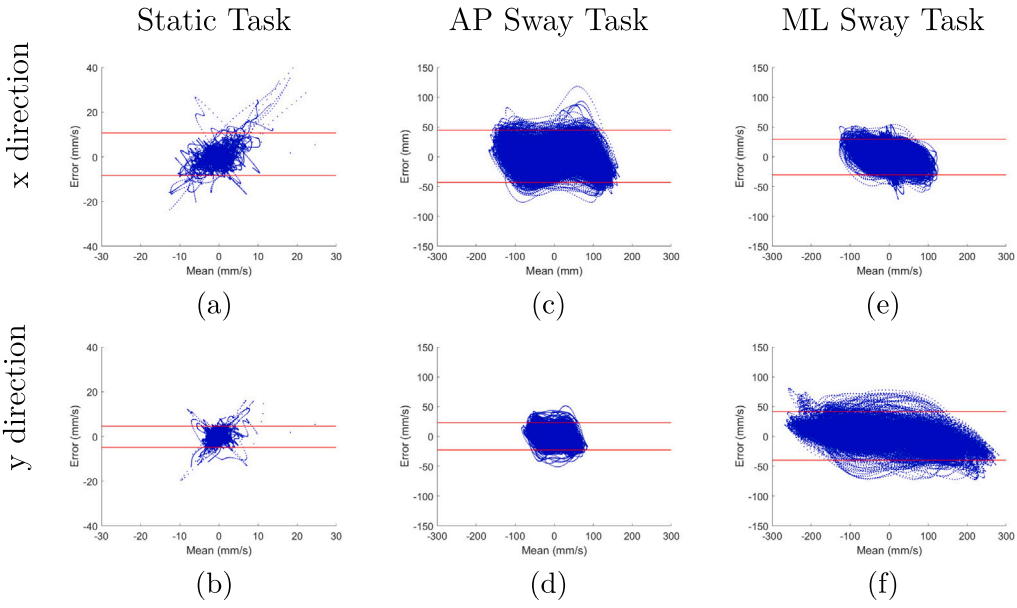

Fig. 6. Bland–Altman plots for velocity.

movement under these conditions. In clinical conditions, the ability to implement straightforward COM estimation methods can reduce the subjective nature of balance evaluations, ultimately improving diagnostic precision and improving care for individuals with conditions that affect postural stability

The markerless system evaluated in this study is composed of a stereoscopic camera and a neural network algorithm that provides a position estimation model of 38 points corresponding to anatomical joints. The VICON system consists of 16 infrared cameras that follow the trajectory of 52 markers placed on the participant to estimate the centres of rotation of the joints and their local coordinate systems. VICON allows the use of the Dumas anthropometric tables, which identifies not only the position of the joint rotation centre but also their related local coordinate systems, from which the COM of each segment is positioned. Note that these COM are not located on the vector joining two centres of rotation of two consecutive joints, which provides a more accurate estimation of the COM. On the other hand, the model provided by the Zed 2i camera only allows us to know the location of the centres of rotation of the joints, which is insufficient to apply the Dumas tables. For this reason, Winter's anthropometric tables are used, which allow the COM of the segments to be located on the vector joining two consecutive joint rotation centres. To assess the level of agreement between both systems, a Bland–Altman analysis was used, obtaining the parameters LOA, RMSE, and R^2.

The Zed 2i camera performance had slight differences between AP and ML tasks. The higher RMSE in the x direction for AP sway can be attributed to the neural network algorithm prioritising the frontal orientation of the torso. On the other hand, the lower RMSE in the non-predominant direction during ML sway highlight the camera better tracking performance in mediolateral movements. Additionally, at the maxima and minima of the sway movements, the error tends to minimise, which means that the peaks and valleys align. However,

when the COM moves between these values, the error increases. This difference could be explained by the use of different models, resulting in two different slopes through the COM motion.

Similar results have been reported in another study using COM displacement estimation to evaluate a multi-camera markerless pose estimation systems during balance related tasks. Chaumeil et al. [38] used a simplified full-body marker set acquired by a 10 camera Qualisys system and a Theia 3D multi-camera markerless pose estimation system to track participants while performing different tasks (walk, lean, beam walking, and counter movement jumps). In this study a Bland–Altman analysis was performed on the estimated COM using Dumas tables, where the LOA values range from 0.58 to 1.40 cm across all tasks. Although most of the movements in this study have a more dynamic nature than those presented in this paper, the reported ranges are consistent with the ranges obtained in the current study.

Other studies have compared markerless and marker based systems during dynamic movements, including gait and sprinting. Needham et al. [37] compared the COM estimation using an open source markerless software (OpenPose) and a full-body marker set, acquired by a multi-camera Qualisys system during sprinting and pushing motions. The reported results included a 95% LOA range −0.037 to 0.046 m for the horizontal displacement of the COM and −1.722 to 1.974 m/s for the horizontal velocity of the COM while sprinting. The high difference ratio between both systems was identified to be the lack of proper neural network training, as there were few training dataset related to the analysed push movement. A similar limitation was also found in our study, where the Zed 2i pose estimation algorithm continuously placed the torso facing front to the camera.

Regarding static trials, although the RMSE and LOA were lower than those computed for sway tasks, the low R^2 value of 0.48 indicates that it is not advisable to use the Zed 2i camera to study the behaviour of the COM in static balance. When the camera is tracking sway movements, the high amplitude of the displacements of the COM estimated by the Zed 2i measurements reduces the influence of the depth error stated above. In contrast, low amplitude displacements in static conditions are more sensitive to the depth estimation errors. This suggests that Zed 2i is not suitable for COM estimation in static balance assessment without additional post-processing algorithms.

The range of motion is another method used to evaluate markerless and marker based systems. Although its use for balance related tasks is limited, since there is minimal movement in such conditions, the conclusions drawn from these analysis can be applied to our study. Galna et al. [55] conducted a study to measure the accuracy of Microsoft Kinect against the gold standard VICON system, to measure movement in people with Parkinson's disease while performing a series of clinically functional movements. While the temporal accuracy provided strong correlation and relative low LOA, spatial accuracy was not as reliable, with the LOA ranging as low as 4% to as high as 146%. This broad difference was particularly high for small movements, which aligns with our own limitations in static balance movement as previously stated.

Regarding velocity, a more erratic behaviour can be observed in static conditions, whereas in sway conditions, despite having a wider LOA, the coefficient of determination R^2 indicates that the velocity estimated by the markerless system maintains a strong correlation with the marker-based system, further strengthening the feasibility of using the Zed 2i camera for dynamic posturography evaluation. Romanato et al. [56] studies the differences in COM velocity between two groups, healthy young adults and patients with Parkinson's disease, using the Romberg test. The COM was estimated using a six camera optoelectronic system and used Dempster tables to estimate the body COM position with a 7-segment model. The reported differences range from a minimum of 1.01 to a maximum of 2.33 mm/s, which is lower than the LOA values obtained in the static tests. This would further indicate that the use of a single Zed 2i camera is not recommended for static balance tests. More research with complementary devices to improve the precision of the data should be done.

Another notable advantage of the Zed 2i camera over other markerless systems concerns data size and the complexity of post-processing. Using a custom Python program, each file generated by the Zed 2i camera's model ranges from 300 KB for static trials up to 900 KB for sway tasks, resulting in a total of approximately 160 MB for 240 trials (30 trials per participant). Once the custom MATLAB script was implemented to analyse these data, post-processing proved straightforward, as the joint keypoints are predefined by the model. In contrast, acquiring data with other multi-camera markerless systems can produce up to 35 GB of video captures for 54 short movement trials [57]. It is also worth emphasising that the Zed 2i camera does not record video, rather, it performs real-time position estimation, thereby avoiding the need to film participants and helping to preserve their privacy.

Regarding the current study limitations, we used a single camera at a fixed position of −10° angle from the sagittal plane for data collection, other research suggests that altering the camera's angle or the participant's orientation can affect the tracking accuracy of the pose estimation algorithm [58]. Verifying such variation lies beyond our current scope, but remains an important consideration for future research. Another challenge relates to the variable sample rate of the recording equipment, which required Zed 2i data interpolation and which could have introduced sampling synchronisation lag. Time normalisation, a widely used strategy in gait analysis, could help reduce these effects [59], but it would require inefficient recurrent validation with the gold standard. Furthermore, advanced post-processing algorithms, such as unscented Kalman filters or Bayesian filters [60], may further refine the keypoint accuracy of the Zed 2i camera model. Finally, specialised neural network architectures trained in biomechanical data, such as convolutional networks tailored for joint identification, hold promise for reducing error ranges and improving reliability in both research and clinical contexts [61].

Although the COM positions were calculated with different anthropometric tables, we believe that the high R^2 and relative low LOA range, compared with other studies, suggests that single camera pose estimation systems show promise for dynamic posturography assessment. These systems offer greater accessibility and adaptability to different environmental conditions, making them suitable for clinical tests. Additionally, they are less invasive than marker-based optoelectronic systems, as they do not require palpation for marker placement.

6. Conclusions

Recently, there has been a growing interest to study the reliability and accuracy of markerless systems due to their reduced invasiveness and lower cost compared to marker-based systems. This study identified that the COM estimated through Winter et al. anthropometric tables using a single Zed 2i camera data during dynamic conditions has a strong correlation with the estimated COM using a marker-based VICON system data and Dumas et al. anthropometric tables. These results indicate that for dynamic posturography assessments, a single Zed 2i camera holds significant promise as a viable alternative to marker-based system.

The LOA ranges for displacement obtained in this study remain consistent with those reported in the literature. Further research should be done to identify if a single Zed 2i camera is enough to identify differences in COM behaviour during clinical balance tests, as this technology reduces data collection as well as processing times, and its portability in addition to low cost allows it to adapt to different environments. Moreover, the use of the Zed 2i respects participant privacy by not recording identifiable video images.

However, static motion tracking shows poor performance. Despite relatively smaller LOA values in the static condition, the low-amplitude

nature of COM movements in static balance magnifies the impact of even small depth estimation errors.

As future work, we propose the use and validation of a multiple Zed 2i cameras array to identify if the COM kinematic behaviour estimation is improved. Although this may increase the overall cost of the system, it would still be a low-cost system compared to other multiple camera systems, enabling a wider range of applications in diagnostics and rehabilitation.

CRediT authorship contribution statement

Ruben Valenzuela: Writing – original draft, Visualization, Software, Methodology, Investigation, Formal analysis, Data curation. **Javier Corral:** Writing – original draft, Visualization, Supervision, Software, Methodology, Investigation, Funding acquisition, Formal analysis, Conceptualization. **Mikel Diez:** Writing – review & editing, Visualization, Supervision, Software, Methodology, Investigation, Funding acquisition, Formal analysis, Data curation, Conceptualization. **Thomas Provot:** Writing – review & editing, Supervision, Software, Formal analysis, Data curation. **Francisco J. Campa:** Writing – review & editing, Validation, Software, Project administration, Methodology, Investigation, Funding acquisition, Data curation, Conceptualization. **Saioa Herrero:** Project administration, Investigation, Funding acquisition, Conceptualization. **Erik Macho:** Validation, Investigation, Funding acquisition, Data curation, Conceptualization. **Charles Pinto:** Project administration, Investigation, Funding acquisition, Conceptualization.

Declaration of competing interest

The authors declare that they have no known competing financial interests or personal relationships that could have appeared to influence the work reported in this paper.

Acknowledgements

Authors would like to thank for the funds received for the project PID2019 105262RB-I00 funded by MCIN/ AEI/10.13039/50110001 1033, for the project PDC2022-133787-I00 funded by MCIN/AEI / 10.13039/501100011033 and by the European Union Next Generation EU/ PRTR, for the project 2018222013 funded by the Basque Government, and STABLE project PID2023-150982OB-I00 funded by MCIU/AEI/10.13039/501100011033/FEDER, UE. Thanks are also addressed for the funds received of the predoctoral grant PRE2020-092455 funded by MCIN/AEI/10.13039/501100011033 and by 'FSE invierte en tu futuro'.

References

[1] Winter DA, Patla AE, Prince F, Ishac M, Gielo-Perczak K. Stiffness control of balance in quiet standing. J Neurophysiol 1998;80:1211–21. http://dx.doi.org/10.1152/jn.1998.80.3.1211.

[2] Keyvanara M, Sadigh MJ, Meijer K, Esfahanian M. A model of human postural control inspired by separated human sensory systems. Biocybern Biomed Eng 2021;41:255–64. http://dx.doi.org/10.1016/j.bbe.2020.12.008.

[3] Beauchet O, Fantino B, Allali G, Muir S, Montero-Odasso M, Annweiler C. Timed up and go test and risk of falls in older adults: A systematic review. J Nutr Heal Aging 2011;15:933–8. http://dx.doi.org/10.1007/s12603-011-0062-0.

[4] de Oliveira CB, Medeiros Ítalo Roberto Torres de, Frota NAF, Greters ME, Conforto AB. Balance control in hemiparetic stroke patients: main tools for evaluation. J Rehabil Res Dev 2008;45:1215. http://dx.doi.org/10.1682/JRRD.2007.09.0150.

[5] Toloza-Cano DC, Zequera M, González GHC. Characterization of the antero-posterior center of pressure in upright position in type 2 diabetics with peripheral diabetic neuropathy and paired healthy controls. Biocybern Biomed Eng 2021;41:306–15. http://dx.doi.org/10.1016/j.bbe.2021.02.001.

[6] Baratto L, Morasso PG, Re C, Spada G. A new look at posturographic analysis in the clinical context: Sway-density versus other parameterization techniques. Mot Control 2002;6:246–70. http://dx.doi.org/10.1123/mcj.6.3.246.

[7] Quijoux F, Nicolaï A, Chairi I, Bargiotas I, Ricard D, Yelnik A, et al. A review of center of pressure (cop) variables to quantify standing balance in elderly people: Algorithms and open-access code*. 2021, http://dx.doi.org/10.14814/phy2.15067.

[8] Paillard T, Noé F. Techniques and methods for testing the postural function in healthy and pathological subjects. 2015, http://dx.doi.org/10.1155/2015/891390.

[9] Hamza MF, Ghazilla RAR, Muhammad BB, Yap HJ. Balance and stability issues in lower extremity exoskeletons: A systematic review. Biocybern Biomed Eng 2020;40:1666–79. http://dx.doi.org/10.1016/j.bbe.2020.09.004.

[10] Corriveau H, Hébert R, Prince F, Raîche M. Postural control in the elderly: An analysis of test-retest and interrater reliability of the cop-com variable. Arch Phys Med Rehabil 2001;82:80–5. http://dx.doi.org/10.1053/apmr.2001.18678.

[11] Schoneburg B, Mancini M, Horak F, Nutt JG. Framework for understanding balance dysfunction in parkinson's disease. Mov Disorders 2013;28:1474–82. http://dx.doi.org/10.1002/mds.25613.

[12] Smith MD, Chang AT, Seale HE, Walsh JR, Hodges PW. Balance is impaired in people with chronic obstructive pulmonary disease. Gait & Posture 2010;31:456–60. http://dx.doi.org/10.1016/j.gaitpost.2010.01.022.

[13] Yu E, Abe M, Masani K, Kawashima N, Eto F, Haga N, et al. Evaluation of postural control in quiet standing using center of mass acceleration: Comparison among the young, the elderly, and people with stroke. Arch Phys Med Rehabil 2008;89:1133–9. http://dx.doi.org/10.1016/j.apmr.2007.10.047.

[14] Doheny EP, McGrath D, Greene BR, Walsh L, McKeown D, Cunningham C, et al. Displacement of centre of mass during quiet standing assessed using accelerometry in older fallers and non-fallers. In: 2012 annual international conference of the IEEE engineering in medicine and biology society. IEEE; 2012, p. 3300–3. http://dx.doi.org/10.1109/EMBC.2012.6346670.

[15] Mazumder O, Tripathy S, Roy S, Chakravarty K, Chatterjee D, Sinha A. Postural sway based geriatric fall risk assessment using kinect. In: 2017 IEEE Sensors. IEEE; 2017, p. 1–3. http://dx.doi.org/10.1109/ICSENS.2017.8234214.

[16] Küng U, Horlings C, Honegger F, Kremer H, Bloem B, van De Warrenburg B, et al. Postural instability in cerebellar ataxia: Correlations of knee, arm and trunk movements to center of mass velocity. Neuroscience 2009;159:390–404. http://dx.doi.org/10.1016/j.neuroscience.2008.11.050.

[17] Dumas R, Chèze L, Verriest JP. Corrigendum to adjustments to mcconville, others, and young, others, body segment inertial parameters [j. biomech. (2006) in press] (doi:10.1016/j.jbiomech.2006.02.013). 2007, http://dx.doi.org/10.1016/j.jbiomech.2006.07.016.

[18] Zatsiorsky VM, King DL. An algorithm for determining gravity line location from posturographic recordings. Technical report, 1998.

[19] Lafond D, Duarte M, Prince F. Comparison of three methods to estimate the center of mass during balance assessment. J Biomech 2004;37:1421–6. http://dx.doi.org/10.1016/S0021-9290(03)00251-3.

[20] Cardarelli S, Mengarelli A, Tigrini A, Strazza A, Nardo FD, Fioretti S, et al. Single imu displacement and orientation estimation of human center of mass: A magnetometer-free approach. IEEE Trans Instrum Meas 2020;69:5629–39. http://dx.doi.org/10.1109/TIM.2019.2962295.

[21] Labrozzi GC, Warner H, Makowski NS, Audu ML, Triolo RJ. Center of mass estimation for impaired gait assessment using inertial measurement units. IEEE Trans Neural Syst Rehabil Eng 2024;32:12–22. http://dx.doi.org/10.1109/TNSRE.2023.3341436.

[22] Winter DA, Patla AE, Ishac M, Gage WH. Motor mechanisms of balance during quiet standing. J Electromyography Kinesiol 2003;13:49–56. http://dx.doi.org/10.1016/S1050-6411(02)00085-8.

[23] Chèze L. Kinematic analysis of human movement. Wiley; 2014, http://dx.doi.org/10.1002/9781119058144.

[24] Fukuchi CA, Fukuchi RK, Duarte M. A public dataset of overground and treadmill walking kinematics and kinetics in healthy individuals, vol. 6, PeerJ; 2018, http://dx.doi.org/10.7717/peerj.4640.

[25] Tesio L, Rota V. The motion of body center of mass during walking: A review oriented to clinical applications. Front Neurol 2019;10. http://dx.doi.org/10.3389/fneur.2019.00999.

[26] Khazzam M, Long JT, Marks RM, Harris GF. Kinematic changes of the foot and ankle in patients with systemic rheumatoid arthritis and forefoot deformity. J Orthop Res 2007;25:319–29. http://dx.doi.org/10.1002/jor.20312.

[27] Kumar D, Wyatt C, Chiba K, Lee S, Nardo L, Link TM, et al. Anatomic correlates of reduced hip extension during walking in individuals with mild-moderate radiographic hip osteoarthritis. J Orthop Res 2015;33:527–34. http://dx.doi.org/10.1002/jor.22781.

[28] Morgan KD, Donnelly CJ, Reinbolt JA. Elevated gastrocnemius forces compensate for decreased hamstrings forces during the weight-acceptance phase of single-leg jump landing: implications for anterior cruciate ligament injury risk. J Biomech 2014;47:3295–302. http://dx.doi.org/10.1016/j.jbiomech.2014.08.016.

[29] Marin MI, Robert S, Sakizlian RE, Rusu L, Rusu RM. A biomechanical evaluation of the upper limb kinematic parameters of the throwing action in handball: A case study. Appl Sci 2024;14:667. http://dx.doi.org/10.3390/app14020667.

[30] Camomilla V, Dumas R, Cappozzo A. Human movement analysis: The soft tissue artefact issue. J Biomech 2017;62:1–4. http://dx.doi.org/10.1016/j.jbiomech.2017.09.001.

[31] Avogaro A, Cunico F, Rosenhahn B, Setti F. Markerless human pose estimation for biomedical applications: a survey. 2023, http://dx.doi.org/10.3389/fcomp.2023.1153160.
[32] Capecci M, Ceravolo MG, Ferracuti F, Grugnetti M, Iarlori S, Longhi S, et al. An instrumental approach for monitoring physical exercises in a visual markerless scenario: A proof of concept. J Biomech 2018;69:70–80. http://dx.doi.org/10.1016/j.jbiomech.2018.01.008.
[33] Gonzalez DRG, Imbiriba LA, Jandre FC. Comparison of body sway measured by a markerless low-cost motion sensor and by a force plate. Res Biomed Eng 2021;37:507–17. http://dx.doi.org/10.1007/s42600-021-00161-4.
[34] Saccenti E, Hendriks MHWB, Smilde AK. Corruption of the pearson correlation coefficient by measurement error and its estimation, bias, and correction under different error models. Sci Rep 2020;10:438. http://dx.doi.org/10.1038/s41598-019-57247-4.
[35] Atkinson G, Nevill AM. Statistical methods for assessing measurement error (reliability) in variables relevant to sports medicine. Sports Med 1998;26:217–38. http://dx.doi.org/10.2165/00007256-199826040-00002.
[36] Wren TA, Isakov P, Rethlefsen SA. Comparison of kinematics between theia markerless and conventional marker-based gait analysis in clinical patients. Gait Posture 2023;104:9–14. http://dx.doi.org/10.1016/j.gaitpost.2023.05.029.
[37] Needham L, Evans M, Cosker DP, Colyer SL. Can markerless pose estimation algorithms estimate 3d mass centre positions and velocities during linear sprinting activities? Sensors 2021;21. http://dx.doi.org/10.3390/s21082889.
[38] Chaumeil A, Lahkar BK, Dumas R, Muller A, Robert T. Agreement between a markerless and a marker-based motion capture systems for balance related quantities. J Biomech 2024;165. http://dx.doi.org/10.1016/j.jbiomech.2024.112018.
[39] Desmarais Y, Mottet D, Slangen P, Montesinos P. A review of 3d human pose estimation algorithms for markerless motion capture. Comput Vis Image Underst 2021;212:103275. http://dx.doi.org/10.1016/j.cviu.2021.103275.
[40] Diego P, Herrero S, Macho E, Corral J, Diez M, Campa FJ, et al. Devices for gait and balance rehabilitation: General classification and a narrative review of end effector-based manipulators. Appl Sci 2024;14:4147. http://dx.doi.org/10.3390/app14104147.
[41] Kanko RM, Laende EK, Davis EM, Selbie WS, Deluzio KJ. Concurrent assessment of gait kinematics using marker-based and markerless motion capture. J Biomech 2021;127:110665. http://dx.doi.org/10.1016/j.jbiomech.2021.110665.
[42] Dumas R, Wojtusch J. Estimation of the body segment inertial parameters for the rigid body biomechanical models used in motion analysis, vol. 1-3, Springer International Publishing; 2018, p. 47–77. http://dx.doi.org/10.1007/978-3-319-14418-4_147.
[43] Winter DA. Biomechanics and motor control of human movement. Wiley; 2009.
[44] Visser J, Nijhuis LO, Janssen L, Bastiaanse C, Borm G, Duysens J, et al. Dynamic posturography in parkinson's disease: diagnostic utility of the first trial effect. Neuroscience 2010;168:387–94. http://dx.doi.org/10.1016/j.neuroscience.2010.03.068.
[45] Grassi L, Rossi S, Studer V, Vasco G, Motta C, Patanè F, et al. Quantification of postural stability in minimally disabled multiple sclerosis patients by means of dynamic posturography: an observational study. J NeuroEngineering Rehabil 2017;14:4. http://dx.doi.org/10.1186/s12984-016-0216-8.
[46] Valenzuela R, Corral J, Diez M, Campa FJ, Herrero S, Macho E, et al. On-screen visual feedback effect on static balance assessment with perturbations. Sensors 2024;24:1588. http://dx.doi.org/10.3390/s24051588.
[47] Association WM. World medical association declaration of helsinki. JAMA 2013;310:2191. http://dx.doi.org/10.1001/jama.2013.281053.
[48] Ortiz LE, Cabrera EV, Gonçalves LM. Depth data error modeling of the zed 3d vision sensor from stereolabs. Electron Lett Comput Vis Image Anal 2018;17:1–15. http://dx.doi.org/10.5565/rev/elcvia.1084.
[49] Nagano A, Komura T, Himeno R, Fukashiro S. Optimal digital filter cutoff frequency of jumping kinematics evaluated through computer simulation. Int J Sport Heal Sci 2003;1:196–201. http://dx.doi.org/10.5432/ijshs.1.196.
[50] Bland JM, Altman DG. Agreement between methods of measurement with multiple observations per individual. J Biopharm Statist 2007;17:571–82. http://dx.doi.org/10.1080/10543400701329422.
[51] Gerke O. Nonparametric limits of agreement in method comparison studies: A simulation study on extreme quantile estimation. Int J Environ Res Public Heal 2020;17:1–14. http://dx.doi.org/10.3390/ijerph17228330.
[52] Scholz JP, Schöner G, Hsu WL, Jeka JJ, Horak F, Martin V. Motor equivalent control of the center of mass in response to support surface perturbations. Exp Brain Res 2007;180:163–79. http://dx.doi.org/10.1007/s00221-006-0848-1.
[53] Nardon M, Pascucci F, Cesari P, Bertucco M, Latash ML. Synergies stabilizing vertical posture in spaces of control variables. Neuroscience 2022;500:79–94. http://dx.doi.org/10.1016/j.neuroscience.2022.08.006.
[54] Crétual A. Which biomechanical models are currently used in standing posture analysis? Neurophysiol Clinique/ Clin Neurophysiol 2015;45:285–95. http://dx.doi.org/10.1016/j.neucli.2015.07.004.
[55] Galna B, Barry G, Jackson D, Mhiripiri D, Olivier P, Rochester L. Accuracy of the microsoft kinect sensor for measuring movement in people with parkinson's disease. Gait & Posture 2014;39:1062–8. http://dx.doi.org/10.1016/j.gaitpost.2014.01.008.
[56] Romanato M, Guiotto A, Volpe D, Sawacha Z. Center of mass-based posturography for free living environment applications. Clin Biomech 2023;104. http://dx.doi.org/10.1016/j.clinbiomech.2023.105950.
[57] Ito N, Sigurðsson HB, Seymore KD, Arhos EK, Buchanan TS, Snyder-Mackler L, et al. Markerless motion capture: What clinician-scientists need to know right now. JSAMS Plus 2022;1:100001. http://dx.doi.org/10.1016/j.jsampl.2022.100001.
[58] D'Haene M, Chorin F, Colson SS, Guérin O, Zory R, Piche E. Validation of a 3d markerless motion capture tool using multiple pose and depth estimations for quantitative gait analysis. Sensors 2024;24:7105. http://dx.doi.org/10.3390/s24227105.
[59] Iosa M, Cereatti A, Merlo A, Campanini I, Paolucci S, Cappozzo A. Assessment of waveform similarity in clinical gait data: The linear fit method. BioMed Res Int 2014;2014. http://dx.doi.org/10.1155/2014/214156.
[60] Begon M, Andersen MS, Dumas R. Multibody kinematics optimization for the estimation of upper and lower limb human joint kinematics: A systematized methodological review. J Biomech Eng 2018;140. http://dx.doi.org/10.1115/1.4038741.
[61] Timmi A, Coates G, Fortin K, Ackland D, Bryant AL, Gordon I, et al. Accuracy of a novel marker tracking approach based on the low-cost microsoft kinect v2 sensor. Med Eng Phys 2018;59:63–9. http://dx.doi.org/10.1016/j.medengphy.2018.04.020.